Michigan State University

National Superconducting Cyclotron Laboratory

BREMSSTRAHLUNG PRODUCTION OF LOW MASS DIELECTRONS IN RELATIVISTIC HEAVY ION COLLISIONS

DIPALI PAL, KEVIN HAGLIN, and DINESH KUMAR SRIVASTAVA

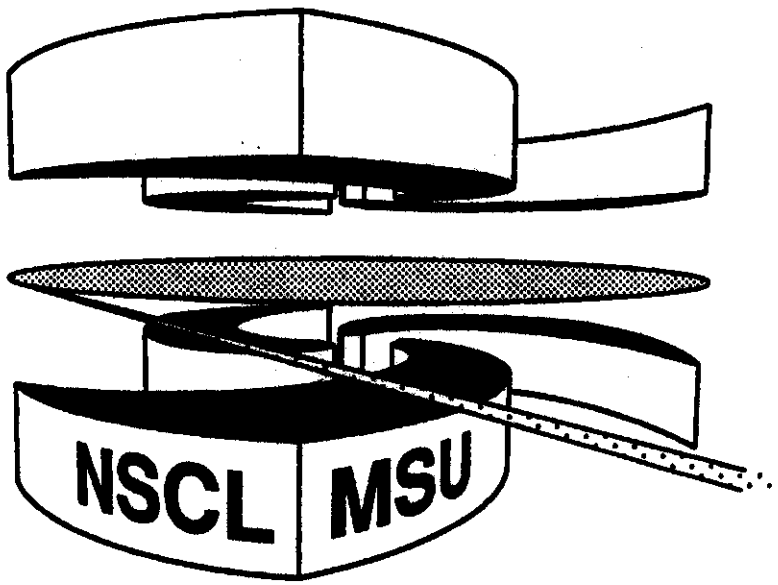

MSUCL-998 **NOVEMBER 1995**

BREMSSTRAHLUNG PRODUCTION OF LOW MASS DIELECTRONS IN RELATIVISTIC HEAVY ION COLLISIONS

Dipali Pal[‡]

Variable Energy Cyclotron Centre, 1/AF Bidhan Nagar, Calcutta 700 064
India

and

Kevin Haglin[§]

National *Superconducting Cyclotron Laboratory*
Michigan *State University, East Lansing*
MI *48824-1321*
U. S. A.

Dinesh Kumar Srivastava*,

Variable Energy Cyclotron Centre, 1/AF Bidhan Nagar, Calcutta 700 064
India

Abstract

The distribution of low mass dielectrons likely to be produced in relativistic heavy ion collisions due to bremsstrahlung processes in quark matter and hadronic matter is obtained. Effort is made to minimize uncertainty and restore Lorentz covariance as compared with past calculations performed in a similar vein. It is found that the excess of dielectrons in $S + Au$ collisions at 200 A GeV measured by the CERES collaboration at CERN - Super Proton Synchrotron may have an important contribution from these processes at very low masses.

PACS numbers: 12.38.Mh, 13.30.Ks, 25.75.+r

‡ E-mail : dipali@veccal.ernet.in
§ E-mail : haglin@nscl.nscl.msu.edu
* E-mall : dks@vecdec.veccal.ernet.in, dinesh@veccal.ernet.in

I INTRODUCTION

Soft photons and dileptons are expected to provide interesting information about all stages of collisions involving heavy nuclei at relativistic energies which are being carried out hoping for an experimental verification of one of the most spectacular predictions of QCD—the existence of quark-gluon plasma (QGP). Low mass dileptons, especially below the pion annihilation threshold, originate from quark-antiquark annihilation and from bremsstrahlung off quarks in QCD matter and pions in hadronic matter[1, 2, 3, 4, 5]. A substantial background to these is provided by the Dalitz decay of π^0 and η mesons. Reactions of the type $\pi\pi \to \rho\gamma^\star$ and $\pi\rho \to \pi\gamma^\star$ should also contribute to low mass dilepton production[6, 7, 8]. The success of the CERES experiment[9] in measuring low mass dielectrons and in estimating the fractional contribution from decay of π^0 and η mesons has provided a unique opportunity to verify the possible occurrence of these radiations which have their origin in a hot and dense, charged medium.

It has also been argued that production of such hot and dense matter is likely accompanied by a rapid transverse expansion of the interacting system during the latest stages. An attempt to get information about the system just before freeze-out by analysing the hadronic distribution may not result in a unique value for a freeze-out temperature or a transverse velocity (see e.g. [10] and references therein). Low mass dileptons can perhaps be used with advantage for this study as their production rate is a very sensitive index of the average temperature of the system and they could be reliable chroniclers of collective flow in the dying moments of the interacting system.

It is also necessary to put these evaluations on firmer footing in view of inconsistencies brought to light by Lichard[11] in almost all treatments of bremsstrahlung production of soft dileptons developed during the last two decades. In the present work we develop the formulation with the correct numerical factors (see later) and with proper accounts of phase space reduction and electromagnetic currents appropriate for the production of virtual photons. Next we estimate the role of bremsstrahlung in the observed excess dielectrons seen by the CERES experiment. We find it to be important.

II FORMULATION

II.1 Soft Photon Approximation for dilepton production

The production of low mass dielectrons (see Ref.[4] for a general discussion) is most conveniently calculated by invoking the soft photon approximation (SPA)[12] wherein the invariant cross section for scattering and at the same time producing a soft real photon of four-momentum q^μ can be written as

$$q_0 \frac{d^4\sigma^\gamma}{d^3q\,dx} = \frac{\alpha}{4\pi^2} \left\{ \sum_{\text{pol}\,\lambda} J\cdot\epsilon_\lambda\, J\cdot\epsilon_\lambda \right\} \frac{d\sigma}{dx} \tag{1}$$

where $d\sigma/dx$ is the strong interaction cross-section for the reaction $ab \to cd$, ϵ_λ is the polarization of the photon, and

$$J^\mu = -Q_a \frac{p_a^\mu}{p_a \cdot q} - Q_b \frac{p_b^\mu}{p_b \cdot q} + Q_c \frac{p_c^\mu}{p_c \cdot q} + Q_d \frac{p_d^\mu}{p_d \cdot q} \tag{2}$$

is the current. The Q's and p's represent the charges (in units of the proton charge) and the particle four-momenta, respectively. Production of soft virtual photons is then obtained by continuing from $q^2 = 0$ to $q^2 = M^2$, where M is the invariant mass of the virtual photon. At this stage, one traditionally writes

$$E_+ E_- \frac{d^6\sigma^{e^+e^-}}{d^3p_+ d^3p_-} = \frac{\alpha}{2\pi^2} \frac{1}{q^2} q_0 \frac{d^3\sigma^\gamma}{d^3q}. \tag{3}$$

Lichard[11] has pointed out that two inaccuracies have already crept into the above formulation. Firstly, the factor $\alpha/2\pi^2$ should be $\alpha/3\pi^2$ so that one respects the natural limiting equality

$$\left(\frac{d\sigma^{\gamma^*}}{d^3q}\right)_M \overset{M \lesssim q_0}{=} \frac{d\sigma^\gamma}{d^3q}\,. \tag{4}$$

Secondly, it is important to use the virtual photon current

$$J^\mu = -Q_a \frac{2p_a^\mu - q^\mu}{2p_a \cdot q - M^2} - Q_b \frac{2p_b^\mu - q^\mu}{2p_b \cdot q - M^2} + Q_c \frac{2p_c^\mu + q^\mu}{2p_c \cdot q + M^2} + Q_d \frac{2p_d^\mu + q^\mu}{2p_d \cdot q + M^2}. \tag{5}$$

Thus, after including these two updates thereby removing earlier inconsistencies, we proceed along the lines of Ref.[4] to write,

$$\begin{aligned} E_+ E_- \frac{d\sigma^{e^+e^-}_{ab\to cd}}{d^3p_+ d^3p_-} &= \frac{\alpha^2}{12\pi^4 M^2} \int |\epsilon \cdot J|^2_{ab\to cd} \frac{d\sigma_{ab\to cd}}{dt} \\ &\qquad \delta(q^2 - M^2)\, dM^2\, \delta^4(q - (p_+ + p_-))\, d^4q\, dt \end{aligned} \tag{6}$$

where the δ functions enforce the energy momentum conservation and t is the four-momentum transfer in the $ab \to cd$ collision. We further perform an average of the electromagnetic factor over photon solid angle before insertion into the above and analogously to Ref.[4], define

$$\hat{\sigma}(s) = \int_{-\lambda(s,m_a^2,m_b^2)/s}^{0} dt \frac{d\sigma_{ab\to cd}}{dt} \left(q_0^2 |\epsilon \cdot J|^2_{ab\to cd}\right). \tag{7}$$

We then write

$$\frac{d\sigma^{e^+e^-}_{ab\to cd}}{dM^2\, d^2M_T\, dy} = \frac{\alpha^2}{12\pi^3 M^2} \frac{\hat{\sigma}(s)}{M_T^2 \cosh^2 y}\,, \tag{8}$$

where M_T is the transverse mass of the dilepton and y is its rapidity, so that, $q_0 = M_T \cosh y$. The expressions are further corrected for neglecting the momentum of the virtual photon in the phase space δ function by including the factor

$$\Phi(s, s_2, m_a^2, m_b^2) = \frac{\lambda^{1/2}(s_2, m_a^2, m_b^2)}{\lambda^{1/2}(s, m_a^2, m_b^2)} \frac{s}{s_2} \tag{9}$$

where $s_2 = s + M^2 - 2\sqrt{s}q_0$ and $\lambda(x,y,z) = x^2 - 2(y+z)x + (y-z)^2$.

Now we can write down the rate of production of dileptons at temperature T using kinetic theory as

$$\frac{dN^{e^+e^-}}{d^4x\,dM^2} = \frac{T^6\,g_{ab}}{16\pi^4}\int_{z_{\min}}^{\infty} dz \int_M^{\sqrt{s}-m_a-m_b} 2\pi\,M_T\,dM_T \int_{-Y}^{Y} dy \frac{\lambda(z^2T^2,m_a^2,m_b^2)}{T^4}\,\Phi(s,s_2,m_a^2,m_b^2)K_1(z)\,\frac{d\sigma_{ab}^{e^+e^-}}{dM^2\,d^2M_T\,dy}, \quad (10)$$

where the limits of integration over the rapidity are obtained from $\lambda(s_2,m_a^2,m_b^2) = 0$. We further have $z_{\min} = (m_a + m_b + M)/T$, $z = \sqrt{s}/T$ and $g_{ab} = N_aN_b(2s_a + 1)(2s_b + 1)$ is the colour and spin degeneracy appropriate for the scattering under consideration. The expressions for angle-averaged electromagnetic factors applied to scattering of two pions, two quarks and quarks plus (massless) gluons are all given in Appendix A.

II.2 Soft Dilepton Production From Quark Matter

A number of processes in quark matter can lead to production of soft dileptons. For emission of soft dileptons from the light (u and d) quarks in QGP we consider bremsstrahlung processes $ab \to ab\gamma^\star$ where a and b are either quarks, antiquarks or gluons. We may remark however, that the higher order QCD processes of the type $q\bar{q} \to \gamma^\star g$ and $q(\bar{q})\,g \to q(\bar{q})\,g\,\gamma^\star$ in the QGP[13], are not important for the masses under consideration. This can be seen by noting that the contribution from these processes, at least for low mass dileptons having high transverse mass M_T, can be written as

$$\frac{dN}{d^4x\,dM^2\,d^2M_T\,dy} \approx \frac{\alpha}{3\pi M^2}\sum e_q^2\frac{\alpha\alpha_s}{2\pi^2}T^2\,e^{-E/T}\ln(ET/m_q^2) \quad (11)$$

where m_q is the thermal mass of the quarks. This contribution becomes small once $M > T$.

In order to evaluate the strong interaction differential cross-sections $d\sigma_{qq}/dt$ and $d\sigma_{qg}/dt$ we have used the phenomenology which was developed in Ref. [14] and subsequently used in Ref. [4] for scattering of quarks and gluons in hot QCD matter;

$$\frac{d\sigma^{ab}}{dt} = C_{ab}\frac{\pi}{2}\,\frac{\alpha_s^2(T)(2t - m_E^2 - m_M^2)^2}{(t-m_E^2)^2(t-m_M^2)^2} \quad (12)$$

where

$$C_{ab} = \begin{cases} 1 & (qg \to qg) \\ \frac{4}{9} & (qq \to qq) \end{cases}, \quad (13)$$

m_E is the colour electrical mass for a baryon-free plasma having two flavours ($N_f = 2$),

$$m_E \approx 4\sqrt{\frac{\pi\alpha_s}{3}}T, \quad (14)$$

and m_M is the colour magnetic mass

$$m_M \approx 5\alpha_s T. \quad (15)$$

We fix the strong coupling constant α_s with

$$\alpha_s(T) = \frac{6\pi}{(33-2N_f)\ln(\kappa T/T_c)}, \tag{16}$$

where $\kappa \approx 8$. In the following we shall fix the transition temperature T_c at 160 MeV.

II.3 Soft Dilepton Production From Hadronic Matter

We shall concentrate on bremsstrahlung production of soft dileptons from processes of the type $\pi\pi \to \pi\pi\gamma^*$. In addition to using the complete electromagnetic factor we use a model for the t dependence of the scattering cross section for pions. For this purpose we include results of a one-boson-exchange calculation approximated with σ, ρ and $f(1270)$ meson exchanges to treat the strong interaction as proposed in Ref. [4] and recently used in a fully covariant and gauge invariant calculation of $\pi\pi \to \pi\pi\, e^+e^-$[15]. Thus the effective Lagrangian which has been used is

$$\mathcal{L}_{\rm int} = g_\sigma \sigma \partial_\mu \vec{\pi} \cdot \partial^\mu \vec{\pi} + g_\rho \vec{\rho}^{\,\mu} \cdot (\vec{\pi} \times \partial_\mu \vec{\pi}) + g_f f_{\mu\nu} \partial^\mu \vec{\pi} \cdot \partial^\nu \vec{\pi}. \tag{17}$$

The following reactions: $\pi^+\pi^- \to \pi^+\pi^-$, $\pi^+\pi^- \to \pi^0\pi^0$, $\pi^+\pi^0 \to \pi^+\pi^0$, and $\pi^-\pi^0 \to \pi^-\pi^0$ have been included. The acceptable level of accuracy of these model calculations has already been displayed[4], and we restate the need for a reliable account of $d\sigma/dt$ for e.g., the $\pi^+\pi^- \to \pi^+\pi^-$ scattering in the following. We note that the differential cross section is proportional to the square of the matrix element describing the overlap of initial and final two-hadron states. This leads to six terms in this matrix element: t and s channel σ-exchange, ρ-exchange and f-exchange processes. The composite nature of mesons calls for a modification at high momentum transfers. This results in an effective suppression in the high momentum regime when the vertices in the t-channel diagrams are given momentum-transfer damping monopole form factors

$$h_\alpha(t) = \frac{m_\alpha^2 - m_\pi^2}{m_\alpha^2 - t}\ , \tag{18}$$

where m_α stands for the mass of the (exchanged) meson σ, ρ, or the f. The treatment also incorporates finite resonance lifetimes into the scalar, vector, and tensor boson propagators. For the f propagator we use,

$$i\mathcal{P}^{\mu\nu\alpha\beta} = \frac{-i\left\{\frac{1}{2}\left(\frac{1}{3}g^{\mu\nu}g^{\alpha\beta} - g^{\mu\alpha}g^{\nu\beta} - g^{\mu\beta}g^{\nu\alpha}\right)\right\}}{k^2 - m_f^2 + im_f\Gamma_f}. \tag{19}$$

Now the full matrix element is given by

$$\mathcal{M} = \mathcal{M}_1 + \mathcal{M}_2 + \mathcal{M}_3 + \mathcal{M}_4 + \mathcal{M}_5 + \mathcal{M}_6, \tag{20}$$

where

$$\mathcal{M}_1 = \frac{-g_\sigma^2 h_\sigma^2(t)(2m_\pi^2 - t)^2}{t - m_\sigma^2 + im_\sigma\Gamma_\sigma}$$

$$
\begin{aligned}
\mathcal{M}_2 &= \frac{-g_\sigma^2(s-2m_\pi^2)^2}{s-m_\sigma^2+im_\sigma\Gamma_\sigma} \\
\mathcal{M}_3 &= \frac{-g_\rho^2 h_\rho^2(t)(s-u)}{t-m_\rho^2+im_\rho\Gamma_\rho} \\
\mathcal{M}_4 &= \frac{g_\rho^2(u-t)}{s-m_\rho^2+im_\rho\Gamma_\rho} \\
\mathcal{M}_5 &= \frac{g_f^2 h_f^2(t)}{t-m_f^2+im_f\Gamma_f}\frac{1}{2}\left(\frac{1}{3}(2m_\pi^2-t)^2-(s-2m_\pi^2)^2-(2m_\pi^2-u)^2\right) \\
\mathcal{M}_6 &= \frac{g_f^2}{s-m_f^2+im_f\Gamma_f}\frac{1}{2}\left(\frac{1}{3}(s-2m_\pi^2)^2-(2m_\pi^2-t)^2-(2m_\pi^2-u)^2\right).
\end{aligned}
\tag{21}
$$

It may be noted that in the above g_σ and g_f are not dimensionless, but $g_\sigma m_\sigma$ and $g_f m_f$ are. The full amplitude is seen to be symmetric under the interchange of the final states as required for bosons. The elastic differential cross section is now obtained as

$$
\frac{d\sigma}{dt} = \frac{|\mathcal{M}|^2}{16\pi s(s-4m_\pi^2)}. \tag{22}
$$

As mentioned earlier the above description is known[4] to give an accurate description of the elastic scattering data. For the sake of completeness we list the values of the parameters: $g_\sigma m_\sigma$=1.85, m_σ = 0.525 GeV, Γ_σ=0.100 GeV, g_ρ=6.15, m_ρ=0.775 GeV, Γ_ρ=0.155 GeV, $g_f m_f$=7.2, m_f=1.274 GeV, and Γ_f=0.176 GeV. The matrix elements for the other reactions are listed in Appendix B.

II.4 Dilepton Production Due to Annihilation Processes in the QGP and Hadronic Matter

Even though the expressions for the contributions of annihilation processes $q\bar{q} \to e^+e^-$ and $\pi^+\pi^- \to e^+e^-$ are well known we shall give them here to fix the notation and to facilitate comparison. The rate for production of dielectrons having an invariant mass M from annihilation of particles having mass m_a is well known[16] to be

$$
\frac{dN}{d^4x\,dM^2} = \frac{\sigma(M)}{2(2\pi)^4}M^3TK_1(M/T)\left[1-\frac{4m_a^2}{M^2}\right] \tag{23}
$$

where

$$
\sigma_\pi(M) = F_\pi(M)\overline{\sigma}(M)(1-4m_\pi^2/M^2)^{1/2}, \tag{24}
$$

$$
\sigma_q(M) = F_q(M)\overline{\sigma}(M), \tag{25}
$$

$$
\overline{\sigma}(M) = \frac{4\pi}{3}\left[1+\frac{2m_e^2}{M^2}\right]\left[1-\frac{4m_e^2}{M^2}\right]^{1/2}, \tag{26}
$$

and

$$
F_q = N_c(2s+1)\sum_f e_f^2 = 8 \quad \text{for u, d, and s quarks,} \tag{27}
$$

and F_π is the pion form-factor. We shall also use $F_{\rm eff}$ in place of F_π to accommodate a host of other reactions[17, 18, 19] which lead to production of dileptons.

II.5 Integration Over the Space-Time History of the System

The dilepton transverse mass yield is then obtained by convoluting the rates for their emission from QGP and from hadronic matter with the space-time history of the system

$$\frac{dN}{dM^2\, d^2M_T\, dy} = \int \tau\, d\tau\, r\, dr\, d\phi\, d\eta \left[f_Q \frac{dN^q}{d^4x\, dM^2\, d^2M_T\, dy} + (1 - f_Q) \frac{dN^\pi}{d^4x\, dM^2\, d^2M_T\, dy} \right], \quad (28)$$

where $f_Q(r, \tau, \eta, \phi)$ gives the fraction of the quark-matter[16] in the system. This expression simplifies considerably for a boost-invariant longitudinal expansion[20], which we shall employ for an initial estimate of these processes. A detailed calculation involving a less restrictive evolution of the system incorporating the transverse expansion is underway and will be published separately.

We consider two situations. In the first case, we perform a model calculation for a central collision of two lead nuclei, which is assumed to lead to the formation of a QGP of u and d quarks and gluons at T_i=200 MeV at initial time $\tau_i = 1$ fm/c. This then expands, cools, and undergoes a first order phase transition to hadronic matter consisting of massless pions at $T = T_c$=160 MeV [massless for these thermodynamics estimates but massive when computing radiation]. When all the matter has converted to pions, it cools further and ultimately freezes out at $T_f = 140$ MeV.

In the second case we consider the situation arising out of central collision of ^{32}S with a target of gold nuclei at the CERN SPS, which was realized in the CERES experiment and which has attracted considerable attention recently[17, 21, 22, 6]. We assume the system has a transverse dimension R_T equal to the radius of a sulphur nucleus and particle rapidity density $dN/dy \approx 225$. Assuming an isentropic expansion we relate the particle rapidity density, the initial temperature T_i and initial time τ_i through[23],

$$T_i^3 \tau_i = \frac{2\pi^4}{45\zeta(3)\, \pi R_T^2 4 a_k} \frac{dN}{dy}, \quad (29)$$

where $a_k = a_Q = 47.5\,\pi^2/90$ if the system is initially in the QGP phase consisting of (massless) u, d and s quarks and of gluons. We model the hadronic phase as consisting of (the complete list of) light pseudoscalar (P) and vector (V) mesons, π, ρ, ω, η, η', ϕ, K, and $K^\star$, where $a_k = a_H \approx 6.8\,\pi^2/90$ [18]. We now assume as before, that this thermalized QGP expands and cools and gets into a mixed phase at the transition temperature $T = T_c$. When all the quark matter has adiabatically converted into hadronic matter, it cools again and freezes out at $T = T_f$. It is well known that $\tau_q = (T_i/T_c)^3\, \tau_i$ gives the proper time at the end of the QGP phase, $\tau_h = r\tau_q$ is the proper time at the end of the mixed phase and $\tau_f = (T_c/T_f)^3\, \tau_h$ gives the time of freeze-out. The parameter $r = 47.5/6.8$ is the ratio of the degrees of

freedom in the QGP to that in hadronic matter and T_f is the freeze-out temperature. For the case of a boost-invariant longitudinal expansion $f_Q = 1$ during the QGP phase, $f_Q = 0$ during the hadronic phase and

$$f_Q(\tau) = \frac{1}{r-1}\left[r\frac{\tau_q}{\tau} - 1\right], \tag{30}$$

during the temporal stretch spanning the region from τ_q to τ_h. We note however that in the earlier cases discussed above $r = 37/3$.

III RESULTS AND DISCUSSIONS

III.1 General Findings

In fig. 1, we give our results for the production rate of dielectrons from quark driven processes. Results are given using a thermal mass as well as a current mass for the quarks. We see that the effect of using the virtual photon current advocated by Lichard[11] is to suppress production by about 20% at lowest invariant mass and using a thermal quark mass. If instead, one uses the current mass for the quarks we see a suppression by a factor of 4–6 at the lowest masses under study. Note the crossover point around 2 and a half times the thermal mass of the quark, a result which has its origin in the angle averaged electromagnetic factor (see Appendix A, Eqs. (1) and (9)) owing to different interference patterns for $M > m$ as compared with $M < m$. The results of Ref.[4] can be obtained from the above by taking the values for the real photon current and multiplying by 3/2.

The results for the pion driven processes are given in fig. 2. We again see a reduction of about 20% in the production of soft dileptons when the virtual photon current of Eq. (5) is used instead of the one for real photons Eq. (2). We can recover[24] the results of Ref.[4] by multiplying the present results using Eq. (2) by 3/2. We shall use the virtual photon current in the electromagnetic factor for all the results to be reported henceforth.

In order to get a general idea of the relative importance of the different mechanisms for production of dielectrons we have plotted (see fig. 3) the contributions for pion annihilation, quark annihilation, quark driven bremsstrahlung and pion driven bremsstrahlung processes to the rate at $T = 160$ MeV. We see that for masses less than 0.3 GeV the bremsstrahlung contribution is rather large. In the case of pions this aspect is further enhanced by the threshold effect of annihilation mechanisms so that neglecting bremsstrahlung contributions for lower masses will not be justified. We should remember that even though the rate for the quark driven bremsstrahlung processes is larger than those for pion driven bremsstrahlung processes, the later contribution is to be multiplied by a much larger space time volume in the expanding system produced in a relativistic heavy ion collision.

This aspect becomes clear by looking at fig. 4 where we present a model calculation for dielectrons produced in a central collision involving two lead nuclei. The system is assumed to be in the form of a QGP initially at $T_i = 200$ MeV and $\tau_i = 1$ fm/c, consisting of u and d quarks, and gluons. The hadronic matter produced

subsequent to hadronization at $T = T_c = 160$ MeV is assumed to consist of (massless) pions and the freeze-out takes place at 140 MeV. Pions are now seen to provide the largest contribution to yields of low mass dielectrons from bremsstrahlung processes. In fact, this contribution is larger than that from quarks even when we take the smallest quark mass (the current mass). This aspect is slightly different from that reported in Ref.[4] (see fig. 13 there), because of the underprediction of the pion contribution due to a numerical error[24], as mentioned earlier.

Finally in fig. 5 we have tried to depict the sensitivity of the production of low mass dielectrons on the freeze-out conditions. We vary the freeze out temperature from 100 MeV to 160 MeV. In the last case the system breaks up right after the mixed phase, without admitting a system of interacting hadrons. We see that the bremsstrahlung production of the low mass dielectrons is large and it is quite sensitive to the value of the freeze-out temperature. In fact, we find that a decrease of 10% in the freeze-out temperature enhances the yield of dielectrons by up to 25%. This sensitivity, especially with regard to the transverse mass distribution, will get considerably magnified when the transverse expansion of the system is included and holds the promise of elevating low mass dielectrons to the status of reliable chroniclers of the last moments of the interacting system. This aspect is under investigation.

We must add that we have not included the Landau-Pomeranchuk-Migdal (LPM) suppression in our estimates. Discussion has been limited to masses larger than $\approx$ 100 MeV, where this suppression is expected to be low[2, 3]. We have also seen that the largest contribution comes from the pions due to the largest four-volume occupied by them in an expansive evolution. During the hadronic phase, the temperature is also rather low which minimizes LPM suppression. Properly treating multiple charge-charge and charge-neutral reactions at arbitrary energies and momentum transfers including a realistic description of the strong-interaction sector is outside the scope of this work, but surely a worthwhile pursuit for future studies.

III.2 $^{32}S + Au$ Collisions at CERN SPS and the CERES Experiment

The CERES experiment[9] at the CERN SPS has produced a measurment of low mass dielectron signals for a number of systems. While the low mass dielectrons for the $p+Be$ and $p+Au$ systems at 450 GeV were found to be consistent with hadronic sources, for the $S + Au$ system at 200 A GeV an enhancement over the hadronic sources by a factor of $5.0 \pm 0.7(\text{stat.}) \pm 2.0(\text{syst.})$ in the mass range $0.2 < M < 1.5$ GeV/c^2 was observed. This result has already attracted a lot of attention. In the following we give our estimate of the contribution of bremsstrahlung processes to the lowest masses for this situation. We have employed a Monte Carlo procedure to account for detector cuts by evaluating the fraction of dielectrons, which satifsfy the requirement that the tranverse momenta of both the electrons are larger than 200 MeV, the opening angle of the two electrons is more than 35 mrad, and that the electrons as well as the pair have $2.1 < \eta < 2.65$ for each M, just as in the CERES experiment[25]. We have limited ourselves to masses above 0.1 GeV/c^2 as

LPM suppression could be quite strong at lower masses [3].

In fig. 6, we give our results for bremsstrahlung yields of dielectrons before incorporating detector cuts in order to know the dominant contribution under slightly different conditions of evolution (the mixed phase will have a shorter duration now, due to a richer composition envisaged for the hadronic matter). We see that the pion driven processes continue to dominate the yield. The relative yields differ with mass for the three curves as there are competing and complicated interference effects whose severity operates as function of reactant masses, charges and dilepton invariant mass owing to the use of the virtual photon current of Eq. (5). It is enough to notice here that thermal quarks modeled as in Eqs. (14) and (15) acquire roughly the same mass as have the pions. Up to an overall shift in yield which depends on specific details of the space time evolution—pions and thermal quarks give the same spectra for masses $.1 < M < .3$ GeV/c^2.

Finally, in fig. 7, we compare our results with the experimental measurements by the CERES group after incorporating the cuts due to the detectors. We limit the comparison to $M < 0.5$ GeV/c^2 as a quantitative description for the data was obtained in Ref.[17] for higher masses and also because the bremsstrahlung contribution at larger masses shuld be small and outside the range of validity of the SPA. We find that the bremsstrahlung contribution gets negligible compared to the hadronic decay background at $M \approx 100$ MeV. At higher masses it is of the order of 20–50% of the excess production of dielectrons seen by the CERES experiment. Of course the largest contribution is visible just below the pion annihilation threshold. We have also shown the results of Srivastava *et al* (SGS) [17] for a comparision. We see that the inclusion of bremsstrahlung processes will certainly improve the description of the data, though a complete description still eludes us. This strengthens the case for inclusion of reactions of the type $\pi\rho \to \pi\gamma^*$ as suggested by the authors of Ref.[17] and first estimated in Ref.[6].

IV SUMMARY

We have obtained the bremsstrahlung production of low mass dielectrons within a soft photon approximation for quark matter and hadronic matter. Care has been taken to eliminate incompleteness of previous and similar calculations due to the numerical factor resulting from computing with a partial leptonic tensor instead of the full expression and due to using real photon currents instead of the more appropriate virtual photon currents in the electromagnetic part of the approximation as pointed out by Lichard[11]. The contributions of pionic processes are found to be large and sensitive to the freeze-out temperature. It is found that an important contribution of these processes may be present in the CERES data above the pion mass and below the two-pion threshold. The sensitivity of these results to the last stages of the evolution hold the promise that it may be possible to utilize low mass dielectrons as chroniclers of the final moments of evolution in relativistic heavy ion collisions.

Acknowledgments

One of us (DKS) would like to thank the hospitality of GSI, Darmstadt where part of this work was done. We would like to thank Jean Cleymans, Axel Drees, Charles Gale, Krzysztof Redlich, Bikash Sinha, Hans J. Specht, Itzhak Tserruya, and Th. Ulrich for many useful discussions during the course of this work. This work was supported in part by the National Science Foundation under grant number PHY-9403666.

APPENDICIES

A ELECTROMAGNETIC FACTOR $|\epsilon \cdot J|^2$ FOR VIRTUAL PHOTONS

We have noted earlier that the use of real-photon current is not completely consistent when evaluating the bremsstrahlung production of soft dileptons. However the angle averaged electromagnetic factor can again be written down for the current involving the virtual photons as before in Ref.[4, 26].

A.1 Results for $m_a = m_b = m_c = m_d = m$

The expression for $m_a = m_b = m_c = m_d = m$ relevant for scattering of equal mass pions or equal mass quarks is given by:

$$\begin{aligned}
|\epsilon \cdot J|^2 \;=\; & \frac{1}{q_0^2}\Bigg\{-\left[\lambda_1^2(Q_a^2+Q_b^2)\frac{4m^2-M^2}{s(1-\beta_a'^2)}+\lambda_2^2(Q_c^2+Q_d^2)\frac{4m^2-M^2}{s(1-\beta_c'^2)}\right] \\
& -2\lambda_1^2 Q_a Q_b(2-\frac{M^2}{s}-\frac{4m^2}{s})F(\vec{\beta}_a',\vec{\beta}_b') \\
& -2\lambda_2^2 Q_c Q_d(2-\frac{M^2}{s}-\frac{4m^2}{s})F(\vec{\beta}_c',\vec{\beta}_d') \\
& +2\lambda_1\lambda_2(Q_aQ_c+Q_bQ_d)\frac{4m^2+M^2-2t}{s}F(\vec{\beta}_a',\vec{\beta}_c') \\
& +2\lambda_1\lambda_2(Q_aQ_d+Q_bQ_c)\frac{2s+M^2-4m^2+2t}{s}F(\vec{\beta}_a',\vec{\beta}_d')\Bigg\} \qquad (1)
\end{aligned}$$

In the above the function

$$F(\vec{x},\vec{y}) = \frac{1}{2\sqrt{R}}\ln\left|\frac{[\vec{x}\cdot\vec{y}-x^2-\sqrt{R}][\vec{x}\cdot\vec{y}-y^2-\sqrt{R}]}{[\vec{x}\cdot\vec{y}-x^2+\sqrt{R}][\vec{x}\cdot\vec{y}-y^2+\sqrt{R}]}\right|, \qquad (2)$$

$$R = (1-\vec{x}\cdot\vec{y})^2-(1-x^2)(1-y^2), \qquad (3)$$

and

$$\lambda_1 = \frac{1}{1-M^2/\sqrt{s}q_0}, \quad \lambda_2 = \frac{1}{1+M^2/\sqrt{s}q_0}. \qquad (4)$$

The velocities β are related to the above definitions through,

$$\beta_a'^2 = \beta_b'^2 = \lambda_1^2\gamma(1-\frac{4m^2}{s}),\ \beta_c'^2 = \beta_d'^2 = \lambda_2^2\gamma(1-\frac{4m^2}{s}) \tag{5}$$

$$\vec{\beta}_a'\cdot\vec{\beta}_b' = -\lambda_1^2(1-\frac{4m^2}{s}),\ \vec{\beta}_c'\cdot\vec{\beta}_d' = -\lambda_2^2(1-\frac{4m^2}{s}), \tag{6}$$

$$\vec{\beta}_a'\cdot\vec{\beta}_c' = -\vec{\beta}_a\cdot\vec{\beta}_d = \lambda_1\lambda_2\gamma(1-\frac{4m^2}{s}+\frac{2t}{s}) \tag{7}$$

with

$$\gamma = 1-\frac{M^2}{q_0^2}. \tag{8}$$

A.2 Results for $m_a = m_c = m$ and $m_b = m_d = 0$

Expressions for the angle averaged electromagnetic factor involving a virtual photon of invariant mass M and relevant for scattering of quarks with massless (and chargeless) gluons are given by

$$\begin{aligned}|\epsilon\cdot J|^2 &= \frac{1}{q_0^2}\left\{-\left[\lambda_1^2Q_a^2\frac{s(4m^2-M^2)}{(s+m^2)^2(1-\beta_a'^2)}+\lambda_2^2Q_c^2\frac{s(4m^2-M^2)}{(s+m^2)^2(1-\beta_c'^2)}\right]\right.\\ &\left.+2\lambda_1\lambda_2Q_aQ_c\frac{s(4m^2+M^2-2t)}{(s+m^2)^2}F(\vec{\beta}_a',\vec{\beta}_c')\right\}.\end{aligned} \tag{9}$$

where the function F is defined as before. However, we now have

$$\lambda_1 = \frac{1}{1-M^2\sqrt{s}/(s+m^2)q_0},\ \ \lambda_2 = \frac{1}{1+M^2\sqrt{s}/(s+m^2)q_0}, \tag{10}$$

and

$$\gamma = 1-\frac{M^2}{q_0^2}. \tag{11}$$

The expressions for the velocities β are now given by,

$$\beta_a'^2 = \lambda_1^2\gamma\frac{(s-m^2)^2}{(s+m^2)^2},\ \ \beta_c'^2 = \lambda_2^2\gamma\frac{(s-m^2)^2}{(s+m^2)^2}, \tag{12}$$

and

$$\vec{\beta}_a'\cdot\vec{\beta}_c' = \lambda_1\lambda_2\gamma\left[1+\frac{2s(t-2m^2)}{(s+m^2)^2}\right]. \tag{13}$$

It is straightforward to show that these expressions for the electromagnetic factor reduce to those of Ref.[4] for $M\to 0$.

B MATRIX ELEMENTS FOR $\pi\pi \to \pi\pi$

Matrix elements for the $\pi^+\pi^- \to \pi^+\pi^-$ scattering has already been given in the text. We list the elements for the other reactions which have been used. First for $\pi^\pm\pi^0 \to \pi^\pm\pi^0$ we have

$$\mathcal{M} = \mathcal{M}_1 + \mathcal{M}_2 + \mathcal{M}_3 + \mathcal{M}_4, \tag{14}$$

where

$$\begin{aligned}
\mathcal{M}_1 &= \frac{-g_\sigma^2 h_\sigma^2(t)(2m_\pi^2 - t)^2}{t - m_\sigma^2 + im_\sigma\Gamma_\sigma} \\
\mathcal{M}_2 &= \frac{-g_\rho^2 h_\rho^2(t)(s-u)}{t - m_\rho^2 + im_\rho\Gamma_\rho} \\
\mathcal{M}_3 &= \frac{g_\rho^2(u-t)}{s - m_\rho^2 + im_\rho\Gamma_\rho} \\
\mathcal{M}_4 &= \frac{g_f^2 h_f^2(t)}{t - m_f^2 + im_f\Gamma_f}\frac{1}{2}\left(\frac{1}{3}(2m_\pi^2 - t)^2 - (s - 2m_\pi^2)^2 - (2m_\pi^2 - u)^2\right).
\end{aligned} \tag{15}$$

Finally, for $\pi^+\pi^- \to \pi^0\pi^0$ we have

$$\mathcal{M} = \mathcal{M}_1 + \mathcal{M}_2 + \mathcal{M}_3 \tag{16}$$

where

$$\begin{aligned}
\mathcal{M}_1 &= \frac{-g_\sigma^2(s - 2m_\pi^2)^2}{s - m_\sigma^2 + im_\sigma\Gamma_\sigma} \\
\mathcal{M}_2 &= \frac{-g_\rho^2 h_\rho^2(t)(s-u)}{t - m_\rho^2 + im_\rho\Gamma_\rho} \\
\mathcal{M}_3 &= \frac{g_f^2}{s - m_f^2 + im_f\Gamma_f}\frac{1}{2}\left(\frac{1}{3}(s - 2m_\pi^2)^2 - (2m_\pi^2 - t)^2 - (2m_\pi^2 - u)^2\right).
\end{aligned} \tag{17}$$

References

[1] C. Gale and J. Kapusta, Phys. Rev. C **35**, 2107 (1987).

[2] J. Cleymans, K. Redlich, and H. Satz, Z. Phys. C **53**, 517 (1991).

[3] J. Cleymans, V. V. Goloviznin, and K. Redlich, Phys. Rev. D **47**, 989 (1993).

[4] K. Haglin, C. Gale, and V. Emel'yanov, Phys. Rev. D **47**, 973 (1993).

[5] P. Koch, Z. Phys. C **57**, 283 (1993).

[6] K. L. Haglin, Michigan State University Report No. MSUCL-978, June 1995.

[7] Charles Gale, private communication.

[8] K. Redlich, private communication.

[9] G. Agakichiev et al., CERES Collaboration, Phys. Rev. Lett. **75**, 1272 (1995).

[10] P. Braun - Munzinger, J. Stachel, J. P. Wessels, and N. Xu, Phys. Lett. B **344**, 43 (1995).

[11] P. Lichard, Phys. Rev. D **51**, 6017 (1995).

[12] R. Rückl, Phys. Lett. B **64**, 39 (1976).

[13] T. Altherr and P. V. Ruuskanen, Nucl. Phys. B **380**, 377 (1992) .

[14] P. Danielewicz and M. Gyulassy, Phys. Rev. D **31** 53 (1985).

[15] H. C. Eggers, R. Tabti, C. Gale and K. Haglin, Report Numbers McGill/95–14, HEPHY–PUB 620/95, MSUCL–974; hep-ph/9510409 and submitted to Phys. Rev. D.

[16] K. Kajantie, J. Kapusta, L. McLerran, and A. Mekijan, Phys. Rev. D **34**, 2746 (1986).

[17] D. K. Srivastava, B. Sinha and C. Gale, Phys. Rev. C, in press.

[18] D. K. Srivastava, J. Pan, V. Emel'yanov, and C. Gale, Phys. Lett. B **329**, 157 (1994).

[19] C. Gale and P. Lichard, Phys. Rev. D **49**, 3338 (1994);
C. Song, C. M. Ko, and C. Gale, Phys. Rev. D **50**, R1827 (1994).

[20] J. D. Bjorken, Phys. Rev. D **27**, 140 (1983).

[21] G. Li, C. M. Ko, and G. E. Brown, Texas A&M University preprint (1995).

[22] W. Cassing, W. Ehehalt, C. M. Ko, Phys. Lett. B **363**, 35 (1995).

[23] R. C. Hwa and K. Kajantie, Phys. Rev. D **32**, 1109 (1985).

[24] The results for pions given in Ref.[4] are too low by a factor of about 2.5 due to a numerical oversight in their computer program. The expressions (for the real photon current) as given there are, however, correct; but for the factor of 2/3 advised by Lichard[11]. We have confirmed this aspect with the authors of Ref.[4].

[25] I. Tserruya, private communication.

[26] J. Zhang, R. Tabti, C. Gale and K. Haglin, Report Numbers McGill–94/56 and MSUCL–961; nucl-th/9501015 and submitted to Phys. Rev. C.

Figure Captions

Figure 1: Consequences of using current for virtual photon in the electromagnetic factor on the bremsstrahlung production of soft dielectrons from the $q\,q(g) \rightarrow q\,q(g)\,\gamma^*$ processes. Results for both, the current quark mass ($\approx$ 5 MeV) and the thermal quark mass are given.

Figure 2: Consequences of using current for virtual photon in the electromagnetic factor on the bremsstrahlung production of soft dielectrons from the $\pi\,\pi \rightarrow \pi\,\pi\,\gamma^*$ processes.

Figure 3: A comparison of rates for thermal processes leading to production of soft dielectrons.

Figure 4: The mass distribution of soft dielectrons from bremsstrahlung processes in the quark matter and hadronic matter, which may be produced in relativistic heavy ion collision of two lead nuclei. We assume the collision to lead to a QGP (of u and d quarks, and gluons) at an intial temperature of T_i at $\tau_i = 1$ fm/c, which then expands, cools, undergoes a first order phase transition to mass-less pions at 160 MeV, and freeze out at 140 MeV.

Figure 5: The dependence of dielectron yield on the freeze-out temperature. The initial conditions are as in fig. 4.

Figure 6: The mass distribution of low mass dielectrons below the pion-annihilation threshold using $T_i \approx 200$ MeV, $T_c = 160$ and $T_f = 140$ MeV corresponding to possible conditions of the CERES experiment for $S + Au$ collisions at CERN SPS. The hadronic matter is assumed to consist of all the light mesons (see text), and the QGP is assumed to consist of u, d, and s quarks, and gluons.

Figure 7: The sum of background from hadron decays and the bremsstrahlung production of dielectrons for the CERES experimnet. The sum of the background from hadron decays and the thermal dielectrons as estimated by the authors of Ref.[17] (labelled SGS), which includes a host of hadronic reactions, ***but not the bremsstrahlung contribution*** is also shown. The thick solid curve gives the hadronic background estimated by the CERES group, and the two short-dashed curves give the upper and the lower limits of the back-ground.

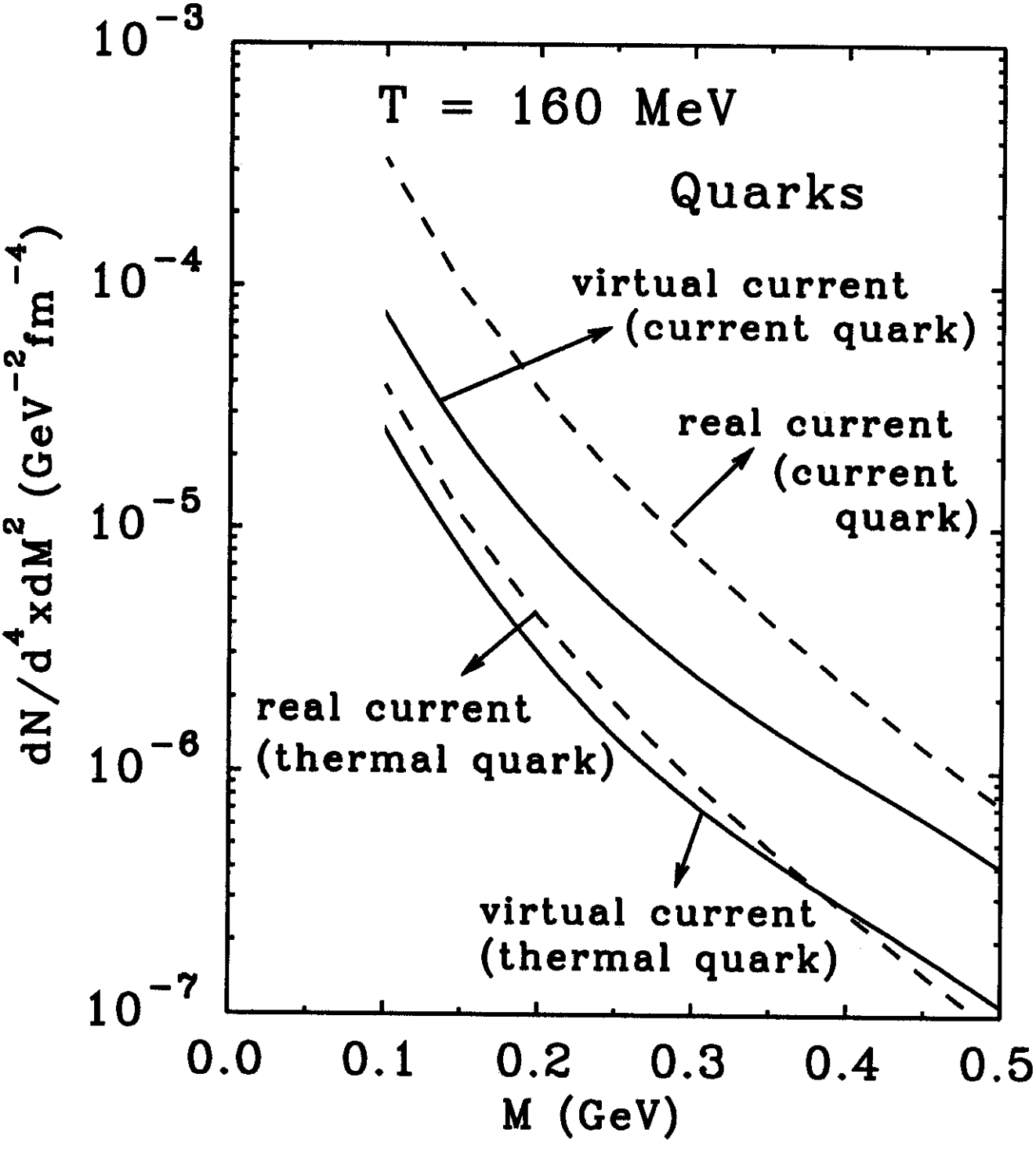
T = 160 MeV
Quarks
virtual current
(current quark)
real current
(current
quark)
real current
(thermal quark)
virtual current
(thermal quark)
10^{-3}
10^{-4}
10^{-5}
10^{-6}
10^{-7}
dN/d^4xdM^2 ($GeV^{-2}fm^{-4}$)
0.0
0.1
0.2
0.3
0.4
0.5
M (GeV)

Figure 1

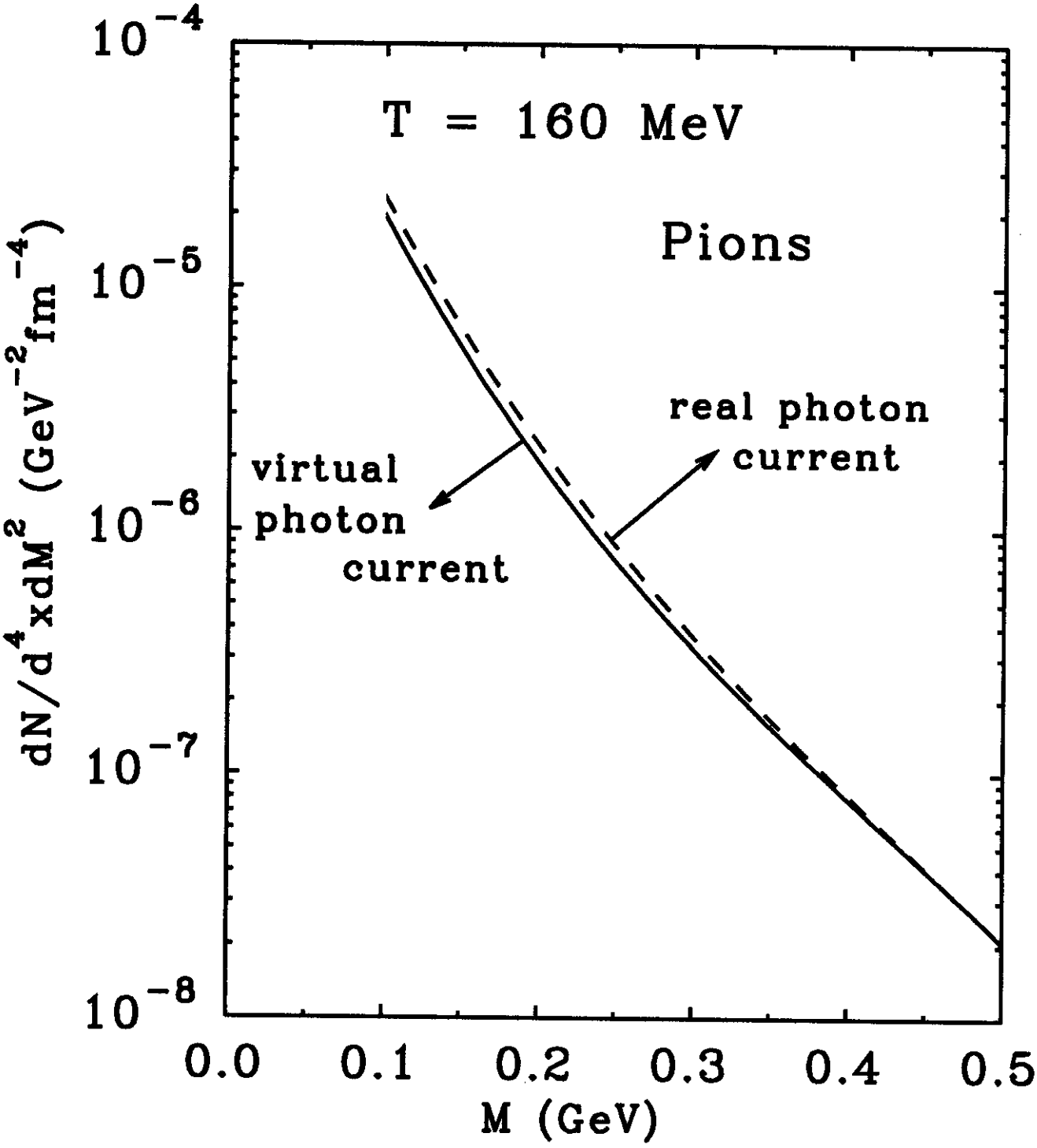
T = 160 MeV
Pions
real photon current
virtual photon current
10^{-4}
10^{-5}
10^{-6}
10^{-7}
10^{-8}
dN/d^4xdM^2 (GeV^{-2}fm^{-4})
0.0
0.1
0.2
0.3
0.4
0.5
M (GeV)

Figure 2

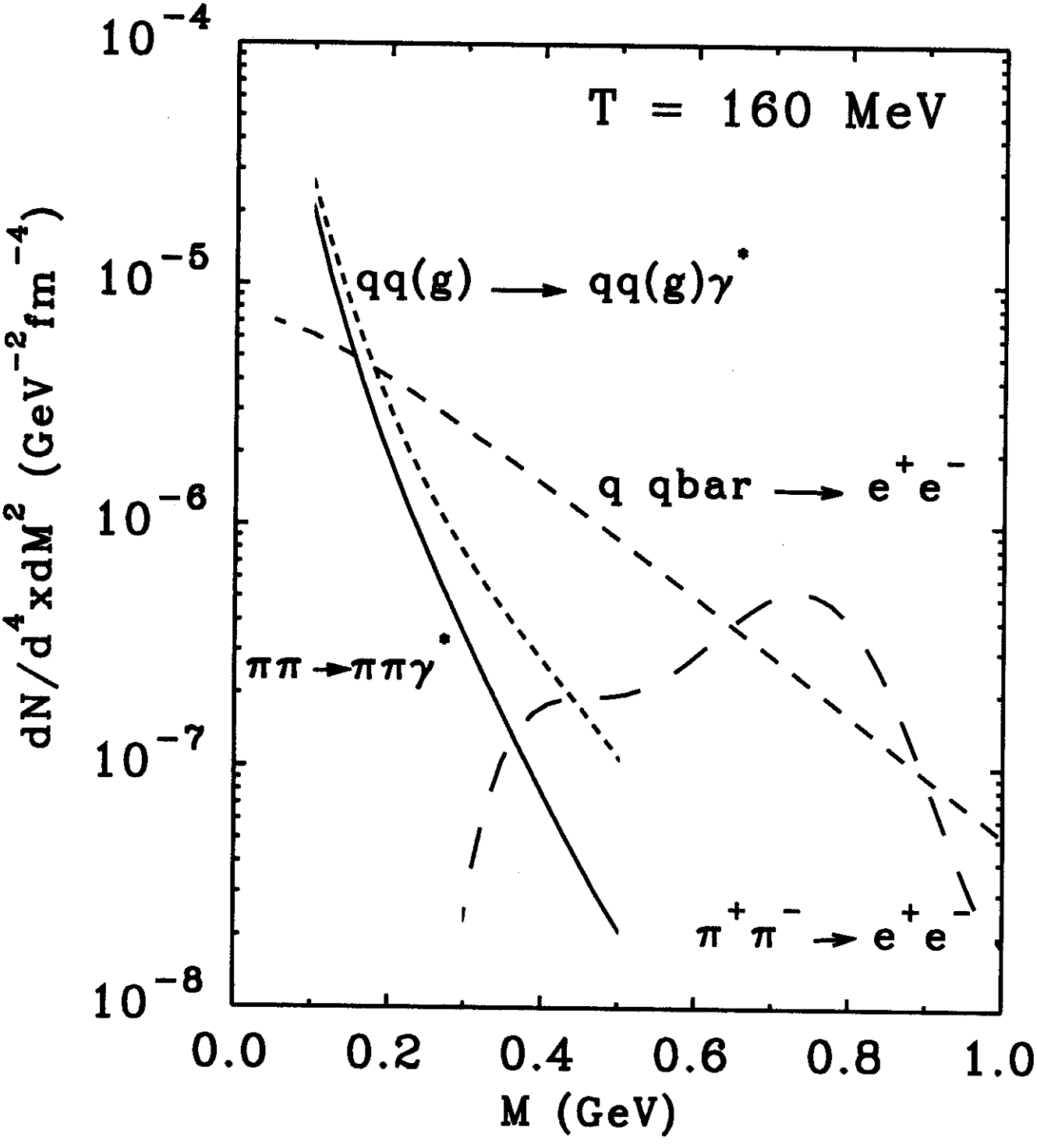
T = 160 MeV
qq(g) → qq(g)γ*
q qbar → e+e-
ππ → ππγ*
π+π- → e+e-
dN/d4xdM2 (GeV-2fm-4)
M (GeV)
10-4
10-5
10-6
10-7
10-8
0.0
0.2
0.4
0.6
0.8
1.0

Figure 3

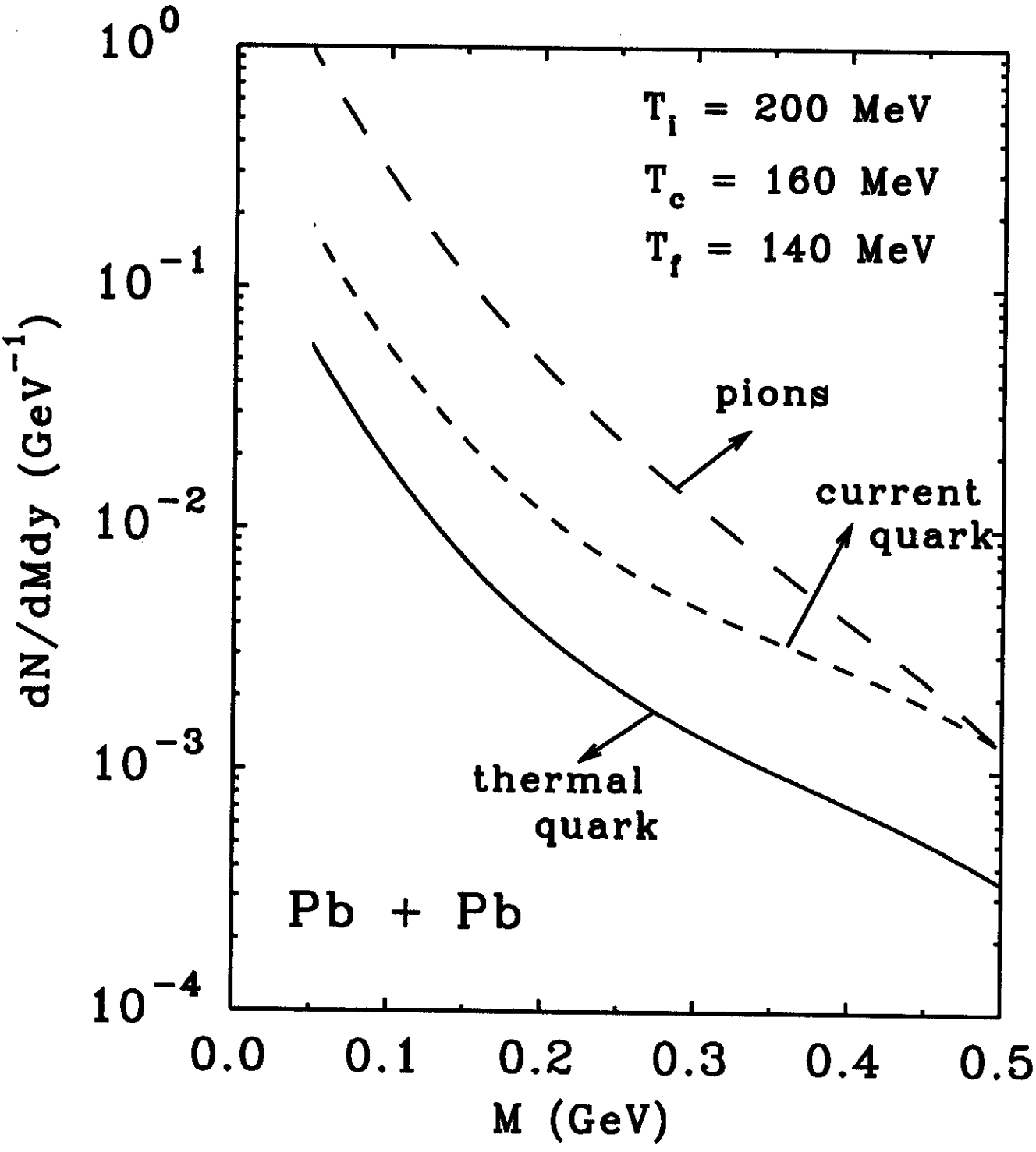
10^0
10^{-1}
10^{-2}
10^{-3}
10^{-4}
dN/dMdy (GeV^{-1})
T_i = 200 MeV
T_c = 160 MeV
T_f = 140 MeV
pions
current quark
thermal quark
Pb + Pb
0.0
0.1
0.2
0.3
0.4
0.5
M (GeV)

Figure 4

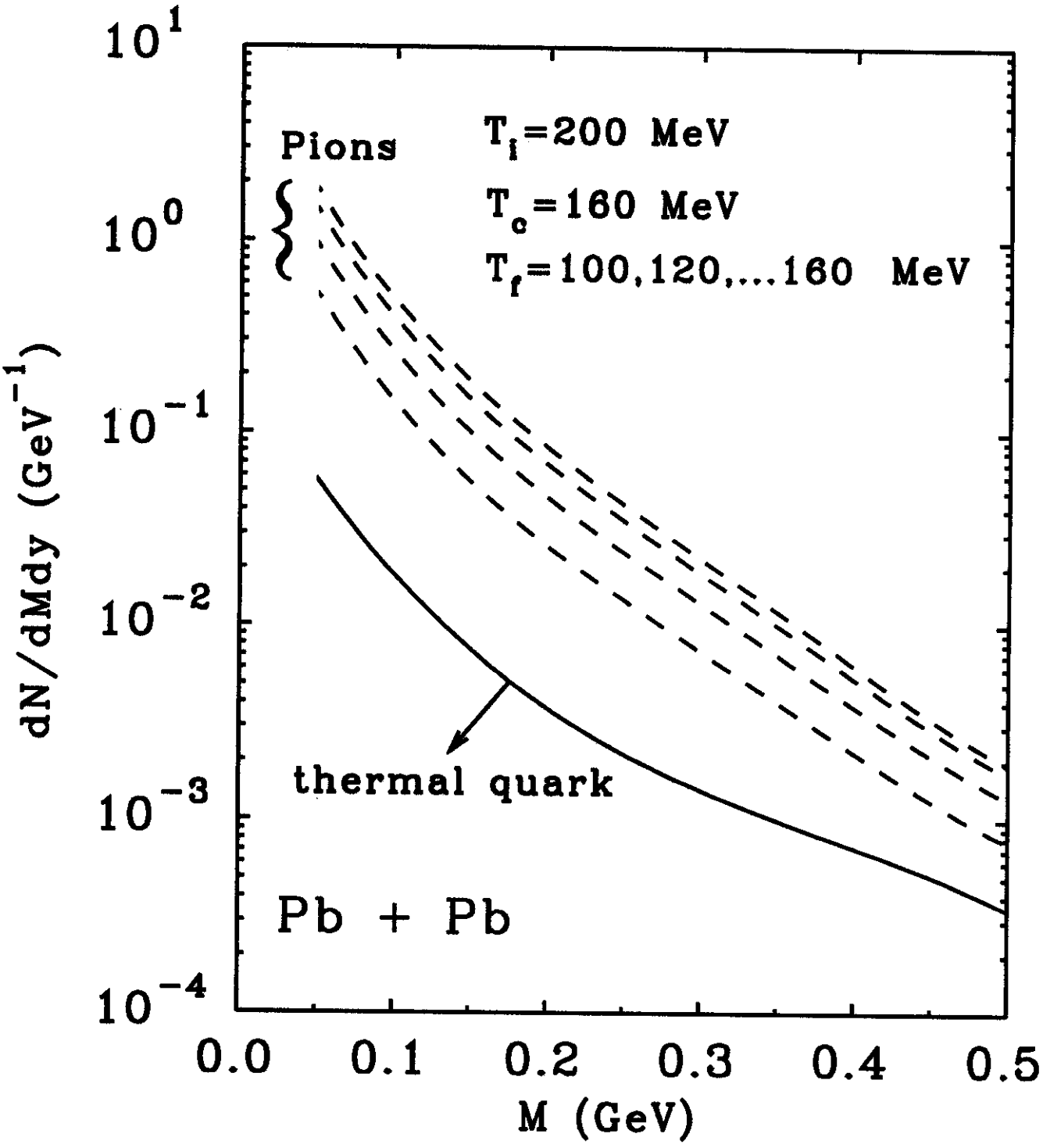
Pions
T_i=200 MeV
T_c=160 MeV
T_f=100,120,...160 MeV
thermal quark
Pb + Pb
dN/dMdy (GeV^{-1})
M (GeV)
10^1
10^0
10^{-1}
10^{-2}
10^{-3}
10^{-4}
0.0
0.1
0.2
0.3
0.4
0.5

Figure 5

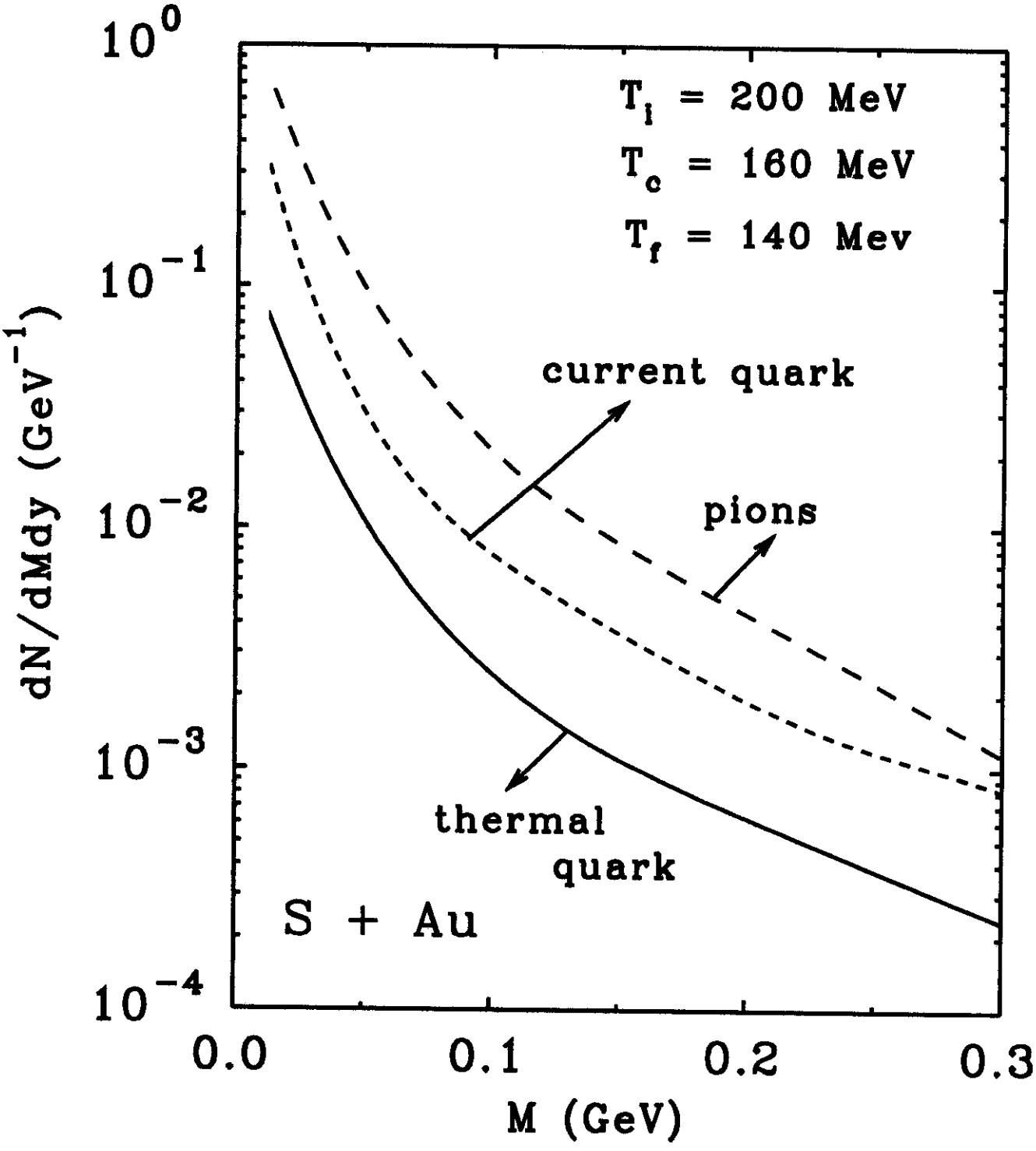
10^0
10^{-1}
10^{-2}
10^{-3}
10^{-4}
dN/dMdy (GeV^{-1})
T_i = 200 MeV
T_c = 160 MeV
T_f = 140 Mev
current quark
pions
thermal
quark
S + Au
0.0
0.1
0.2
0.3
M (GeV)

Figure 6

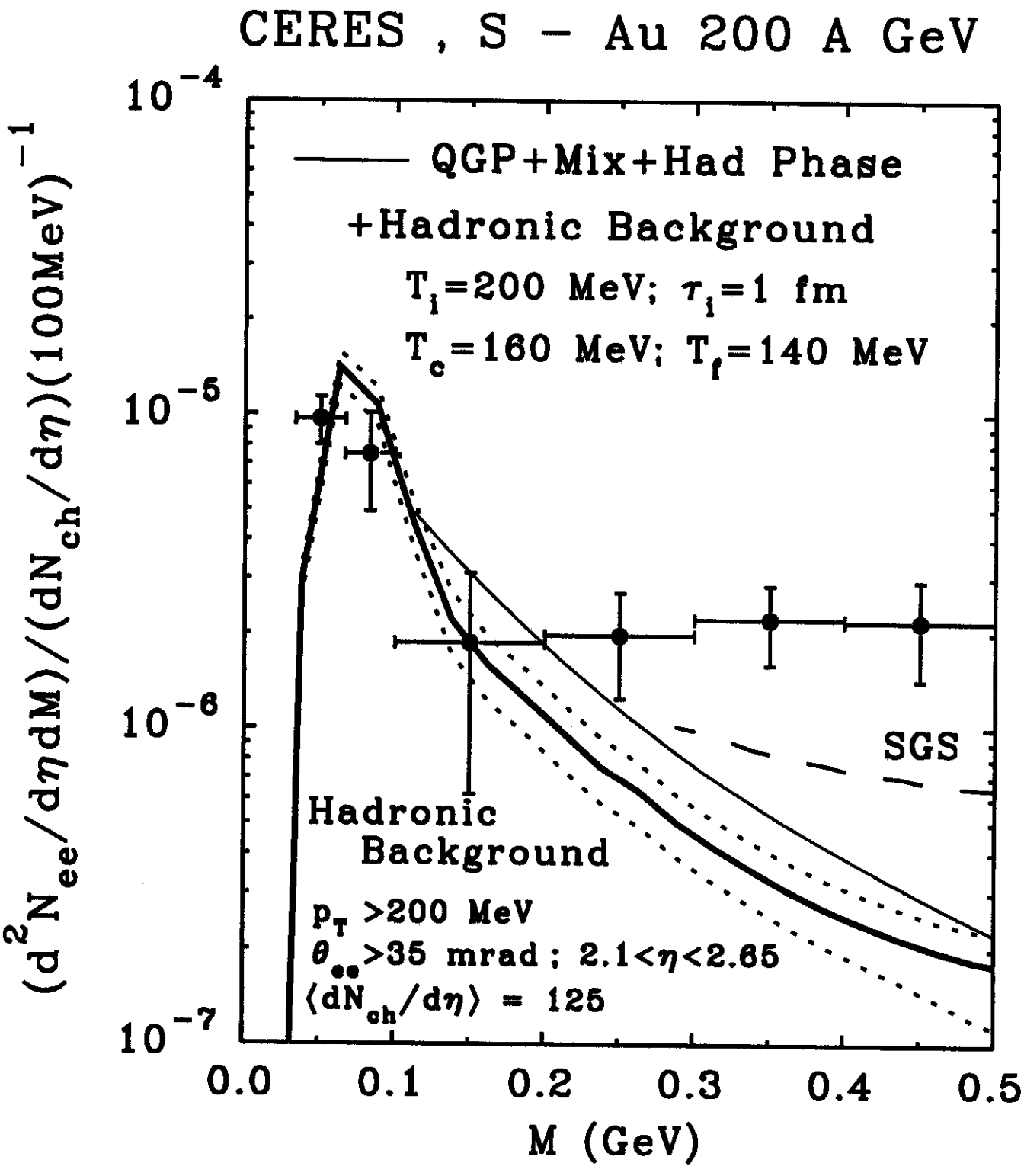
CERES , S – Au 200 A GeV
QGP+Mix+Had Phase
+Hadronic Background
T_i=200 MeV; τ_i=1 fm
T_c=160 MeV; T_f=140 MeV
SGS
Hadronic
Background
p_T >200 MeV
θ_{ee}>35 mrad ; 2.1<η<2.65
$\langle dN_{ch}/d\eta \rangle$ = 125
$(d^2N_{ee}/d\eta dM)/(dN_{ch}/d\eta)(100MeV)^{-1}$
M (GeV)
10^{-4}
10^{-5}
10^{-6}
10^{-7}
0.0
0.1
0.2
0.3
0.4
0.5

Figure 7